Giovanni Finocchio,[1,*]

Main contributors: Riccardo Tomasello,[2] Anna Giordano[1]

Other contributors: Vito Puliafito,[1] Giulio Siracusano,[1] Bruno Azzerboni,[1] Mario Carpentieri[3]

[1]University of Messina, Italy - *for any queries please about this report contact gfinocchio@unime.it

[2]University of Perugia, Italy

[3] Politecnico di Bari, Italy

Introduction

The standard *Problem #5* has been used to benchmark our self-implemented micromagnetic solver[1,2], petaspin[3] , which includes the spin-transfer torque originated from a current flowing through a ferromagnet in presence of a magnetic texture.

Geometry, material parameters, initial state and applied current

We have carefully followed the indications proposed in the standard *Problem #5*. We simulated a rectangular magnetic material with dimensions 100 nm × 100 nm × 10 nm, aligned with the *x*, *y*, *z* axes of a Cartesian coordinate system, with origin at the center of the film. We used two discretization cells: (*i*) 2.5 nm × 2.5 nm × 2.5 nm, and (*ii*) 1.25 nm × 1.25 nm × 1.25 nm.

The material parameters used are the same as the ones in the standard *Problem #5*:

Saturation Magnetization M_s: 800 kA/m

Exchange constant A: 13 pJ/m

Anisotropy constant K: 0 J/m^3

Gilbert damping parameter α: 0.1

Gilbert gyromagnetic ratio γ_0: 2.21×10^5 m/(As).

The initial state is created and relaxed to the equilibrium as indicated in the standard *Problem #5*. In this way, we achieve the equilibrium vortex configuration, as shown in Fig. 1 for the discretization cells (*i*) and (*ii*).

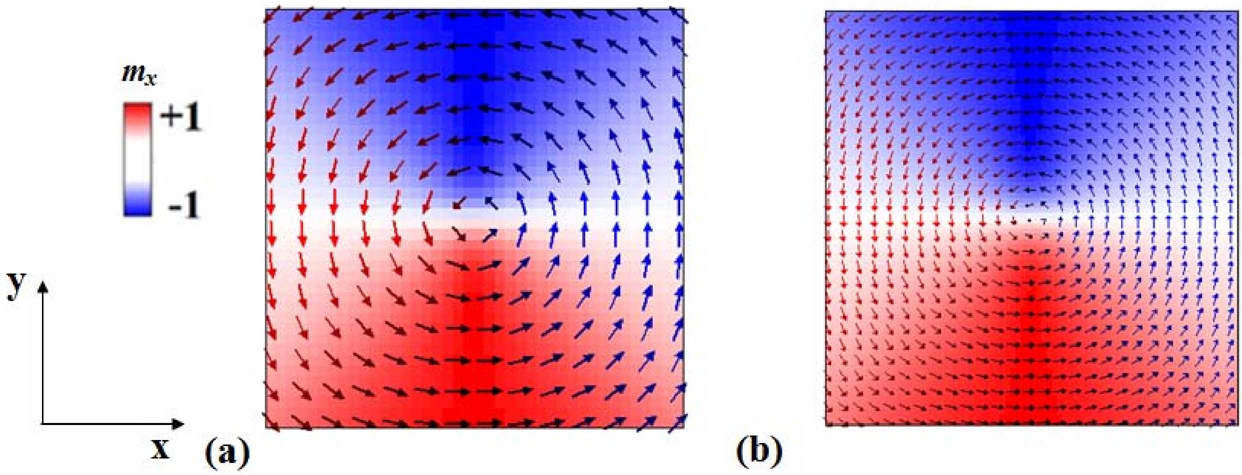

Fig. 1: Spatial distribution of the magnetization corresponding to the equilibrium vortex configuration as obtained by our micromagnetic simulations for the discretization cells (a) 2.5 nm × 2.5 nm × 2.5 nm, and (b) 1.25 nm × 1.25 nm × 1.25 nm. The background colors are related to the reduced *x*-component of the magnetization (blue negative, red positive), while the colors of the arrows refer to the reduced *y*-component of the magnetization (blue positive, red negative). The Cartesian coordinate system is also indicated.

The in-plane current is applied along the *x*-direction such that the product of the polarization rate *P* and current density j_{FE} is equal to -10^{12} A/m^2, as proposed in the standard *Problem #5*.

Boundary conditions

Since outside of the magnetic material, the applied current is not polarized, we need to introduce proper boundary conditions, as stated in the standard *Problem #5*. In detail, at the surfaces where the current enters and leaves the magnetic material, the spin-transfer torque must be zero. This is an important point to successfully benchmark our solver. Therefore, we neglect the spin-transfer torque for the first and last column of cells in both case (*i*) and (*ii*) (see Fig. 2).

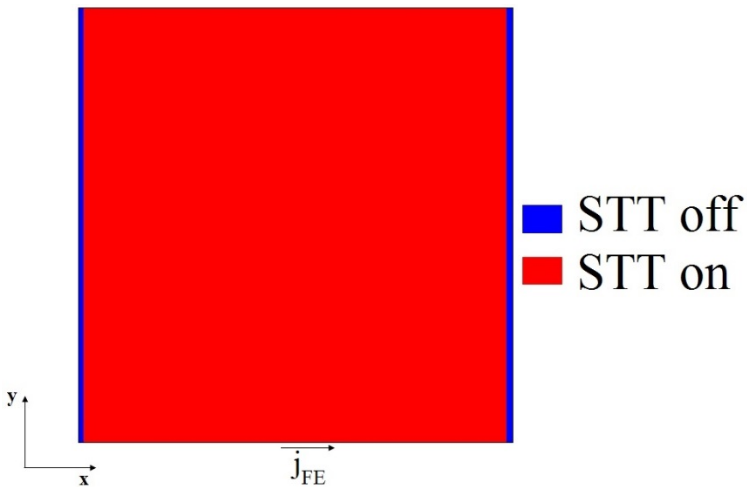

Fig. 2: Example of boundary conditions for the applied current for case (*ii*). The blue columns indicate the cells where the spin-transfer torque is neglected.

Spin Torque Dynamics

We consider the dimensionless form of the LLG equation corresponding to Equation (5) in the standard *Problem #5*:

$$\frac{d\mathbf{m}}{d\tau} = -\mathbf{m}\times\mathbf{h}_{\mathbf{EFF}} + \alpha\mathbf{m}\times\frac{d\mathbf{m}}{d\tau} + \frac{\mu_B P \mathrm{j}_{\mathrm{FE}}}{\gamma_0 e M_S^2}\frac{d\mathbf{m}}{dx} - \frac{\mu_B P \mathrm{j}_{\mathrm{FE}}}{\gamma_0 e M_S^2}\beta\mathbf{m}\times\frac{d\mathbf{m}}{dx} \tag{1}$$

where $\mathbf{m} = \mathbf{M}/M_s$ is the reduced magnetization, $\tau = \gamma_0 M_s t$ is the dimensionless time, $\mathbf{h}_{\mathbf{EFF}}$ is the normalized effective magnetic field, which includes the exchange, magnetostatic, anisotropy and external fields, $\mu_B = 9.274\times10^{-24}$ J/T is the Bohr magneton, $e = 1.60\times10^{-19}$ C is the electron charge, and β is the non-adiabatic parameter.

By making simple calculations, we obtain:

$$\frac{d\mathbf{m}}{d\tau}(1+\alpha^2) = -\mathbf{m}\times\mathbf{h}_{\mathbf{EFF}} - \alpha\mathbf{m}\times\mathbf{m}\times\mathbf{h}_{\mathbf{EFF}} + u(\alpha-\beta)\mathbf{m}\times\left(\frac{d\mathbf{m}}{dx}\right) - u\left(1+\alpha\beta\right)\mathbf{m}\times\mathbf{m}\times\left(\frac{d\mathbf{m}}{dx}\right) \tag{2}$$

where $u = \frac{\mu_B P \mathrm{j}_{\mathrm{FE}}}{\gamma_0 e M_S^2}$. Given the material parameters, and multiply by $\gamma_0 M_s$, independently of β, we obtain $u_T = \gamma_0 M_s u = 72.45$ m/s.

We have obtained the following solutions, by considering the two discretization cells (i) and (ii) and by changing the non-adiabatic parameter accordingly with the standard *Problem #5*, i.e. $\beta = 0,\ 0.05,\ 0.1,\ 0.5$.

RESULTS with discretization 2.5 nm × 2.5 nm × 2.5 nm.

- $\beta = 0$

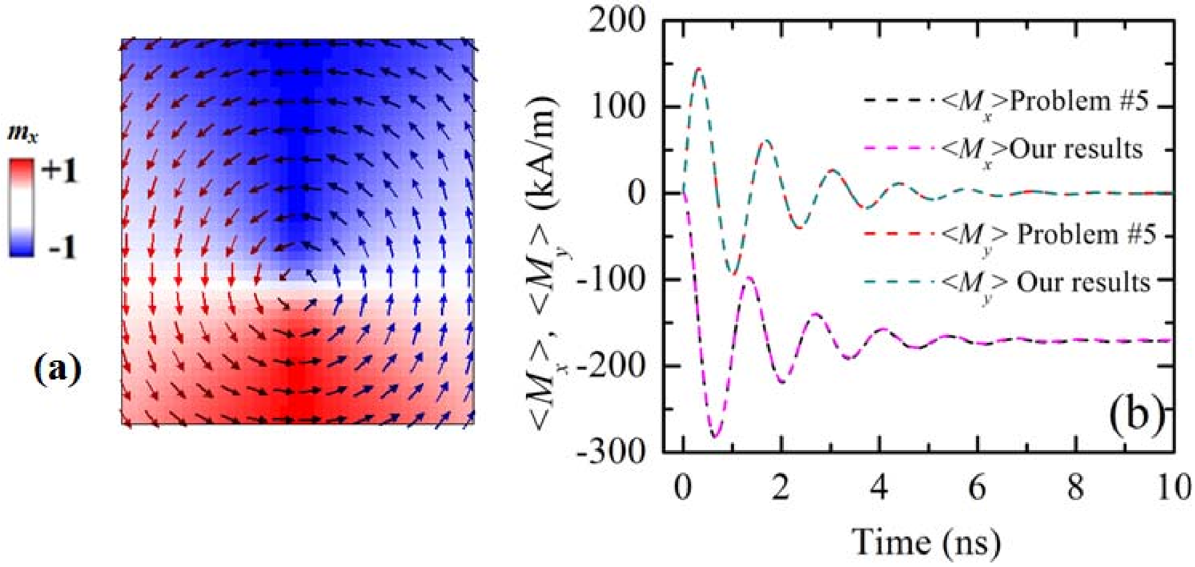

Fig. 3: (a) spatial distribution of the magnetization corresponding to the final vortex state, and (b) time evolution of the three magnetization components as obtained by our micromagnetic simulations for the discretization cells 2.5 nm × 2.5 nm × 2.5 nm, and $\beta = 0$, compared with the ones of the standard *Problem #5*. In (a), the background colors are related to the reduced *x*-component of the magnetization (blue negative, red positive), while the colors of the arrows refer to the reduced *y*-component of the magnetization (blue positive, red negative). In (b), the black and red dashed lines refer to the *x*- and *y*- magnetization components of the standard *Problem #5* respectively, the magenta and green dashed lines refer to the *x*- and *y*- magnetization components, respectively, as obtained by our micromagnetic simulations.

- $\beta = 0.05$

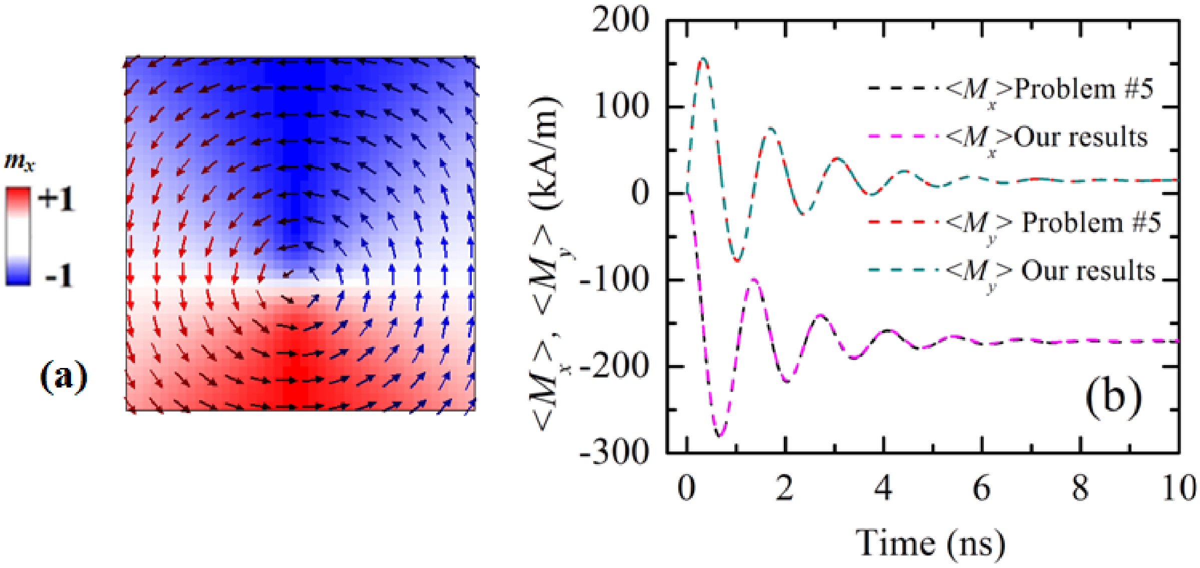

Fig. 4: (a) spatial distribution of the magnetization corresponding to the final vortex state, and (b) time evolution of the three magnetization components as obtained by our micromagnetic simulations for the discretization cells 2.5 nm × 2.5 nm × 2.5 nm, and $\beta = 0$, compared with the ones of the standard *Problem #5*. In (a), the background colors are related to the reduced *x*-component of the magnetization (blue negative, red positive), while the colors of the arrows refer to the reduced *y*-component of the magnetization (blue positive, red negative). In (b), the black and red dashed lines refer to the *x*- and *y*- magnetization components of the standard *Problem #5* respectively, the magenta and green dashed lines refer to the *x*- and *y*- magnetization components, respectively, as obtained by our micromagnetic simulations.

- $\beta = 0.1$

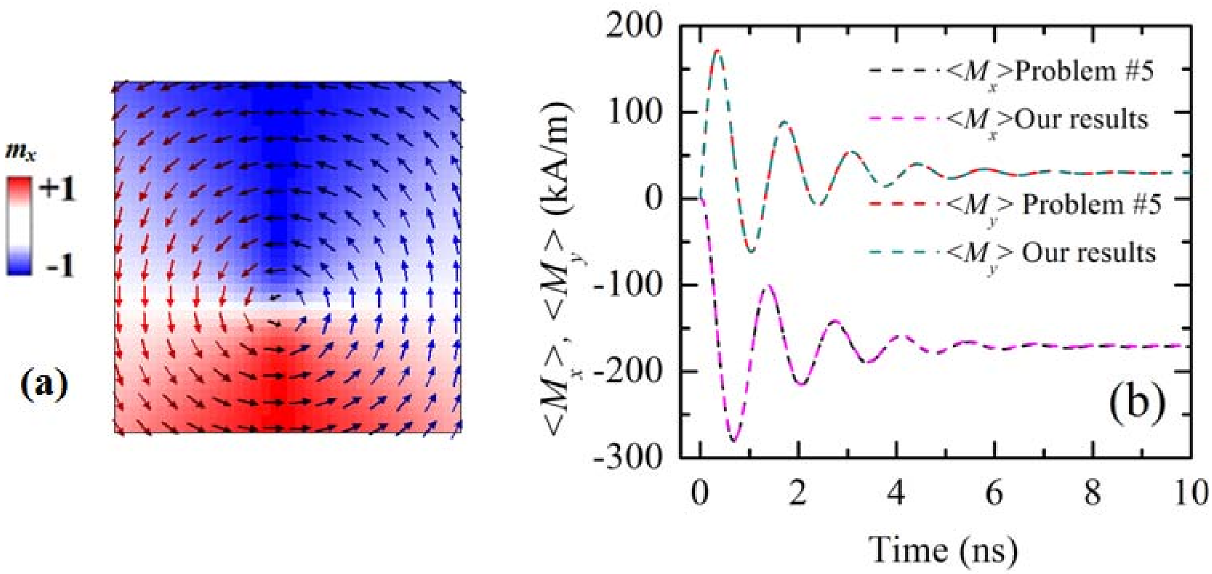

Fig. 5: (a) spatial distribution of the magnetization corresponding to the final vortex state, and (b) time evolution of the three magnetization components as obtained by our micromagnetic simulations for the discretization cells 2.5 nm × 2.5 nm × 2.5 nm, and $\beta = 0$, compared with the ones of the standard *Problem #5*. In (a), the background colors are related to the reduced *x*-component of the magnetization (blue negative, red positive), while the colors of the arrows refer to the reduced *y*-component of the magnetization (blue positive, red negative). In (b), the black and red dashed lines refer to the *x*- and *y*- magnetization components of the standard *Problem #5* respectively, the magenta and green dashed lines refer to the *x*- and *y*- magnetization components, respectively, as obtained by our micromagnetic simulations.

- $\beta = 0.5$

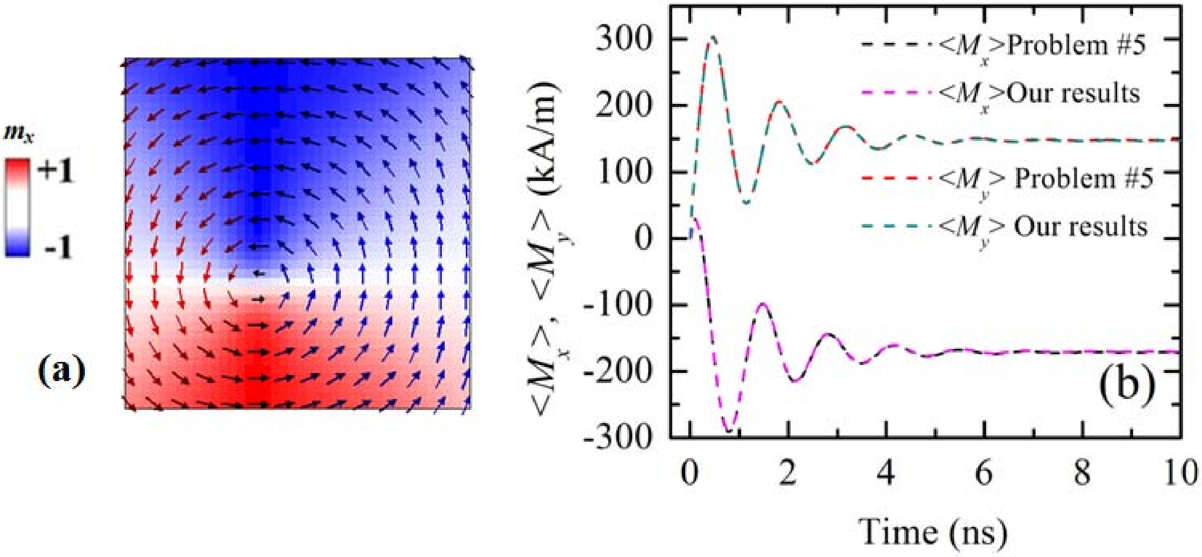

Fig. 6: (a) spatial distribution of the magnetization corresponding to the final vortex state, and (b) time evolution of the three magnetization components as obtained by our micromagnetic simulations for the discretization cells 2.5 nm × 2.5 nm × 2.5 nm, and $\beta = 0$, compared with the ones of the standard *Problem #5*. In (a), the background colors are related to the reduced *x*-component of the magnetization (blue negative, red positive), while the colors of the arrows refer to the reduced *y*-component of the magnetization (blue positive, red negative). In (b), the black and red dashed lines refer to the *x*- and *y*- magnetization components of the standard *Problem #5* respectively, the magenta and green dashed lines refer to the *x*- and *y*- magnetization components, respectively, as obtained by our micromagnetic simulations.

RESULTS with discretization 1.25 nm × 1.25 nm × 1.25 nm.

- $\beta = 0$

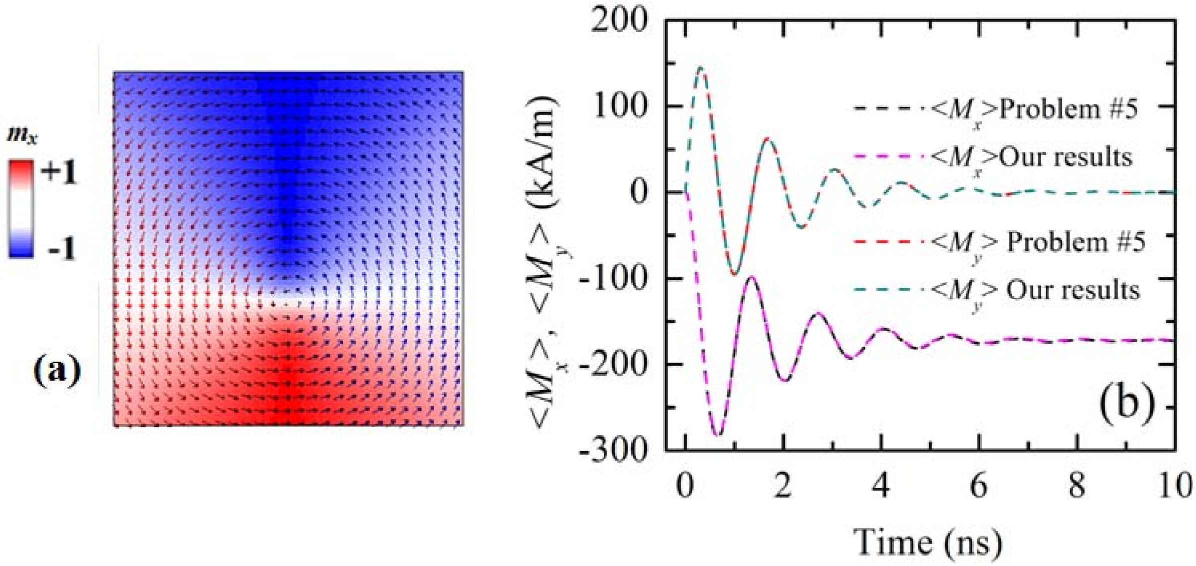

Fig. 7: (a) spatial distribution of the magnetization corresponding to the final vortex state, and (b) time evolution of the three magnetization components as obtained by our micromagnetic simulations for the discretization cells 1.25 nm × 1.25 nm × 1.25 nm, and $\beta = 0$, compared with the ones of the standard *Problem #5*. In (a), the background colors are related to the reduced *x*-component of the magnetization (blue negative, red positive), while the colors of the arrows refer to the reduced *y*-component of the magnetization (blue positive, red negative). In (b), the black and red dashed lines refer to the *x*- and *y*- magnetization components of the standard *Problem #5* respectively, the magenta and green dashed lines refer to the *x*- and *y*- magnetization components, respectively, as obtained by our micromagnetic simulations.

- $\beta = 0.05$

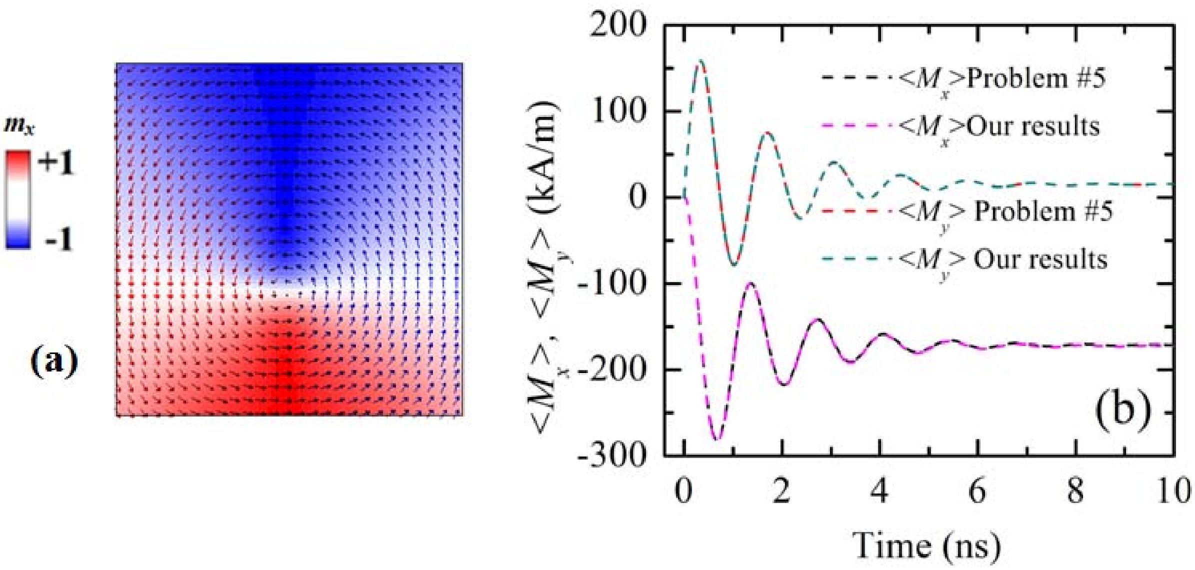

Fig. 8: (a) spatial distribution of the magnetization corresponding to the final vortex state, and (b) time evolution of the three magnetization components as obtained by our micromagnetic simulations for the discretization cells 1.25 nm × 1.25 nm × 1.25 nm, and $\beta = 0$, compared with the ones of the standard *Problem #5*. In (a), the background colors are related to the reduced *x*-component of the magnetization (blue negative, red positive), while the colors of the arrows refer to the reduced *y*-component of the magnetization (blue positive, red negative). In (b), the black and red dashed lines refer to the *x*- and *y*- magnetization components of the standard *Problem #5* respectively, the magenta and green dashed lines refer to the *x*- and *y*- magnetization components, respectively, as obtained by our micromagnetic simulations.

- $\beta = 0.1$

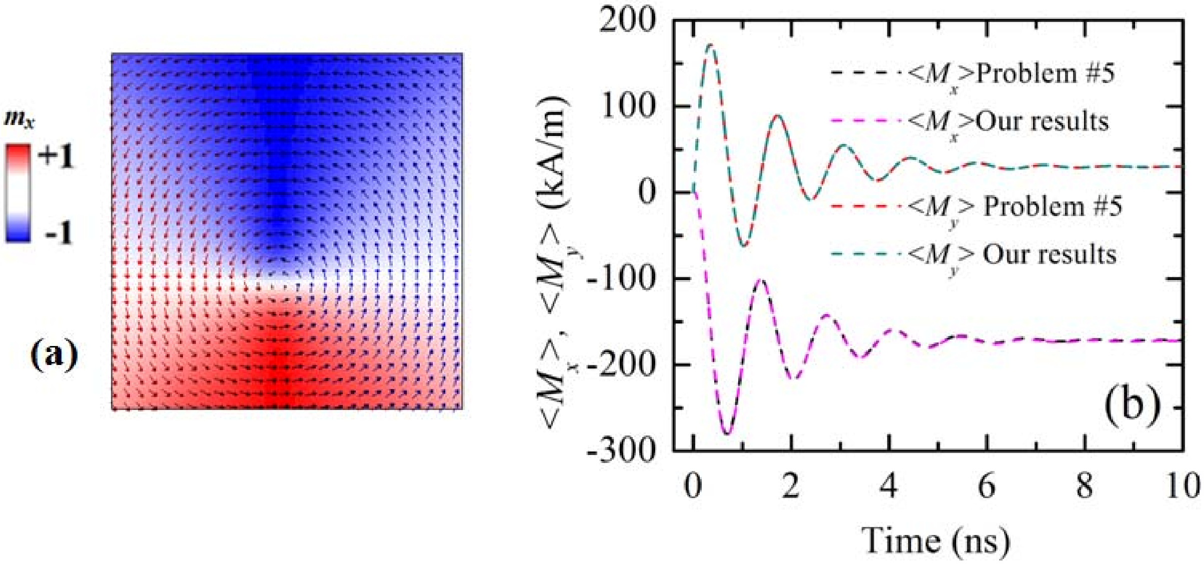

Fig. 9: (a) spatial distribution of the magnetization corresponding to the final vortex state, and (b) time evolution of the three magnetization components as obtained by our micromagnetic simulations for the discretization cells 1.25 nm × 1.25 nm × 1.25 nm, and $\beta = 0$, compared with the ones of the standard *Problem #5*. In (a), the background colors are related to the reduced *x*-component of the magnetization (blue negative, red positive), while the colors of the arrows refer to the reduced *y*-component of the magnetization (blue positive, red negative). In (b), the black and red dashed lines refer to the *x*- and *y*- magnetization components of the standard *Problem #5* respectively, the magenta and green dashed lines refer to the *x*- and *y*- magnetization components, respectively, as obtained by our micromagnetic simulations.

- $\beta = 0.5$

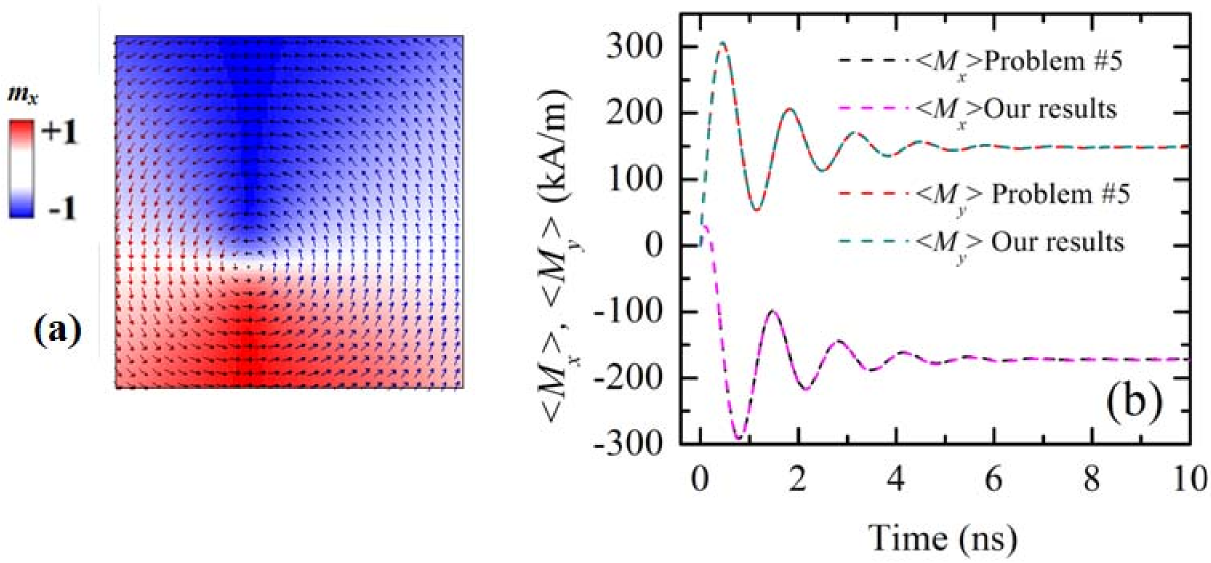

Fig. 10: (a) spatial distribution of the magnetization corresponding to the final vortex state, and (b) time evolution of the three magnetization components as obtained by our micromagnetic simulations for the discretization cells 1.25 nm × 1.25 nm × 1.25 nm, and $\beta = 0$, compared with the ones of the standard *Problem #5*. In (a), the background colors are related to the reduced *x*-component of the magnetization (blue negative, red positive), while the colors of the arrows refer to the reduced *y*-component of the magnetization (blue positive, red negative). In (b), the black and red dashed lines refer to the *x*- and *y*- magnetization components of the standard *Problem #5* respectively, the magenta and green dashed lines refer to the *x*- and *y*- magnetization components, respectively, as obtained by our micromagnetic simulations.

References

[1] L. Lopez-Diaz, D. Aurelio, L. Torres, E. Martinez, M. a Hernandez-Lopez, J. Gomez, O. Alejos, M. Carpentieri, G. Finocchio, and G. Consolo, J. Phys. D. Appl. Phys. **45**, 323001 (2012).

[2] A. Giordano, G. Finocchio, L. Torres, M. Carpentieri, and B. Azzerboni, J. Appl. Phys. **111**, 07D112 (2012).

[3] Extention of GPMagnet." [Online]. Available: http://www.goparallel.net